Mechanics of Materials 15 (1993) 99–115
Elsevier

Fundamental aspects of brittle cooperative phenomena – Effective continua models

Dusan Krajcinovic, Vlado Lubarda [1] and Dragoslav Sumarac [2]

Mechanical and Aerospace Engineering, Arizona State University, Tempe, AZ 85287-6106, USA

Received 13 March 1992; revised version received 3 November 1992

The present paper focuses on the study of some of the fundamental aspects of the cooperative brittle phenomena and damage growth. This rather complex problem is studied on a simple discretized artifice known as the parallel bar model. The disorder in microstructure is introduced by a statistical description of the distribution of the link rupture strengths. The criteria of the damage growth are derived from the thermodynamic analysis of the rupturing process. Stability analysis of the damage growth is also presented. The paper discusses different damage measures and corresponding conjugate affinities.

1. Introduction

Depending on circumstances brittle rupture in a typical material with disordered microstructure may occur in one of several different modes. In this study the attention is focused on the case when rupture occurs as a result of a cooperative action of a diffuse population of microcracks. More specifically, the considered deformation process may be interpreted as a *gradual dilution* of the microstructure of a solid reflecting nucleation of new and growth of the already existing microcracks. On the specimen scale this process is observed and measured as the degradation of specimen transport properties (macro stiffness or, less rigorously, elastic moduli). Of special interest is the infinitely short interval during which a continuous process on the microscale (gradual dilution) causes an abrupt, discontinuous and qualitative change of the macro response (loss of the specimen stiffness or macro failure in a load controlled test).

In actual engineering solids the inelastic deformation processes are to a large extent characterized by disorder on the microscale. The micro-defects randomly scattered over a large part of the volume are, additionally, random in shape and size as well. This is especially true during the initial phase of the deformation process. In the course of loading a semblance of order is induced by the prevailing stress field in terms of preferential directions of damage growth. At macro failure a large number of defects self organizes into a cluster spanning the specimen from one end to the other reducing its stiffness to zero.

The evolution of damage in disordered microstructures is obviously not a simple, deterministic process admitting careless application of conventional continuum models formulated originally for considerations of ductile phenomena. In general, crack growth will commence when the available elastic energy release rate exceed the material toughness at the crack tip. Hence, the damage evolution (defined here as formation of new internal surfaces in the material through the process of cracking) depends on the coincidence of local stress concentration (hot spots) and re-

Correspondence to: Prof. D. Krajcinovic, Department of Mechanical and Aerospace Engineering, College of Engineering and Applied Sciences, Arizona State University, Tempe, AZ 85287-6106, USA.

[1] Permanent address: Mechanical Engineering Department, University of Montenegro, Podgorica, Yugoslavia.

[2] Permanent address: Civil Engineering Department, University of Belgrade, Belgrade, Yugoslavia.

gions of inferior toughness (weak links) of the microstructure. Fracture toughness is, generally, a random function of coordinates and its scatter depends on the material itself, previous history and defects attributable to manufacturing processes. The energy release rate for the observed crack is an integrated quantity which, nevertheless, depends on the adjacent microdefects and microstructure as well. Thus, in the case of many microcracks estimates of their individual growth are quantified by a continuum measure of damage representing expectations of the growth of the entire ensemble of microcracks. In order to be useful this measure must be physically identifiable and measurable in tests.

Analytical modeling of this process is, for obvious reasons, fraught by pitfalls and open to ambiguity. For the most part these pitfalls are proportional to the complexities of the cumbersome mathematical structure of non-deterministic models claiming both rigor and generality. A bevy of different continuum damage models, often pretentious and seldom rigorous (Krajcinovic, 1984), is a testimony to this state of affairs.

To clarify some of the fundamental aspects of the physics of damage evolution it is helpful to start with models characterized by simple mathematical structures. Simplification in modeling is typically achieved through discretization. A truss or a grid is, for example, one of the rudimentary approximations of a solid. The parallel bar system is an even simpler computational artifice which was, nevertheless, extensively and successfully used in the past to model both ductile (Iwan, 1967; Lubarda et al., 1992) and brittle (Krajcinovic and Silva, 1982; Hult and Travnicek, 1982, etc.) phenomena. Historically, the first application of the parallel bar in applied mechanics was used to estimate the rupture strength of cables (Daniels, 1945).

A parallel bar model emphasizes parallel connection of N links (bars, bonds). Each end of the system links is provided by a rigid beam (bus) ensuring equal elongation of links during the deformation process. A parallel bar system may be considered as being either a loose or a tight bundle depending on the manner in which the externally applied tensile load F is shared by the links. In a loose bundle system the external load F is shared equally by all extant links regardless of their relative position within the system. In contrast, to describe the local load fluctuations in dependence of the position of defects within a tight bundle system it is necessary to prescribe a local load sharing rule.

2. Loose bundle parallel bar system

Consider first the simplest approximation of a perfectly brittle solid by a loose bundle parallel bar system assuming that:

(i) all extant links share equally in carrying the external tensile load F regardless of their position within the system;
(ii) all N links have identical stiffness $k = K/N$ and elongations u;
(iii) all links remain elastic until they rupture; and
(iv) the rupture strength f_r of links is a random variable defined by a prescribed probability density distribution $p(f_r)$.

Application of a loose bundle parallel bar system implicitly assumes that the damage evolution and ultimately the failure are attributable primarily to the existence of the regions of inferior toughness within the material. Local stress concentrations are, therefore, assumed to have a second-order effect on the structural response. It is worth mentioning that the parallel bar model is the discrete version of the popular self-consistent model based on the assumptions identical to these listed above (Krajcinovic, 1989).

During the deformation of the system subjected to a quasistatically incremented external tensile load F the tensile forces in individual links f_i ($i = 1$ to N) keep increasing. When the force f_i in a link exceeds its strength f_{ri} the link ruptures releasing its force. The released force is distributed quasistatically and equally to all extant links. Consequently, the deformation process is characterized by the sequential ruptures of individual links. On the system scale rupture of individual links is observed as a gradually decreasing (system) stiffness.

Since each link is perfectly elastic until it ruptures, the force–displacement relation for the ith link is

$$f_i = Ku/N = ku, \quad \text{if} \quad 0 \leqslant ku \leqslant f_{ri},$$

and

$$f_i = 0, \quad \text{if} \quad ku \geqslant f_{ri}. \tag{2.1}$$

The equilibrium equation for the system is then

$$F = \sum_{i=1}^{N} f_i = Ku\left(1 - \frac{n}{N}\right) = Ku(1 - D), \tag{2.2}$$

where n is the number of ruptured links (at a given magnitude of the externally applied tensile force F). On the micro-scale the number of ruptured links n suffices to define the recorded history. The fraction of ruptured links

$$D = n/N, \tag{2.3}$$

is a physically appealing measure of the recorded history, in this case accumulated damage, on the macro-scale. In absence of ductile phenomena and residual strains, D fully defines the state of the material and quantifies the level of degradation of the material stiffness and, perhaps, even the residual load bearing capability. The deformation of the system is fully defined by two variables u and D.

For a very large number of links N a given property can be treated as being equal to its expectation. For instance, $p(f_r)\,\mathrm{d}f_r$ is the probability that the rupture strength f_{ri} can be found within the interval $[f_r, f_r + \mathrm{d}f_r]$. Thus, the damage parameter (2.3) rewritten as

$$D = \int_{f_{\min}}^{ku} p(f_r)\,\mathrm{d}f_r = \mathrm{prob}(f_r < ku) = P(ku), \tag{2.4}$$

is actually the cumulative probability function $P(ku)$ of the given rupture strength probability density function $p(f_r)$. In (2.4) $f_{\min}$ is the rupture strength of the weakest link (Fig. 1). As shown in Krajcinovic and Silva (1982), the reliability function reflecting the chance that the system will survive the level of force Ku is $(1 - D)$, while the instantaneous failure (hazard) rate that the system which survived the same force will fail immediately thereafter is $p(ku)/(1 - D)$.

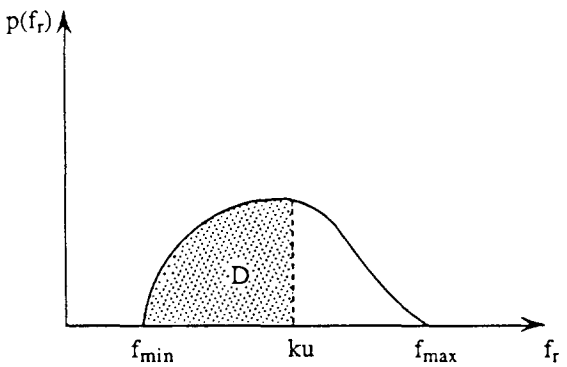

Fig. 1. Rupture strength probability function $p(f_r)$. $f_{\min}$ and $f_{\max}$ are the rupture strengths of the weakest and strongest link. The damage variable D is the cumulative probability corresponding to current displacement level u.

It is interesting to point out that (2.4) represents the damage evolution law, i.e., the constitutive relation relating damage and elongation. The incremental form of (2.4) is

$$\mathrm{d}D = p(ku)k\ \mathrm{d}u = p(u)\ \mathrm{d}u. \tag{2.5}$$

Therefore, once the distribution of rupture strengths $p(f_r)$ on the microscale is known, the damage evolution law can be derived in contrast to being a priori and arbitrarily postulated.

Maximum force to which the system can be subjected (i.e., macro failure in a force-controlled test) occurs when the tangent modulus reduces to zero, i.e., when

$$\frac{\mathrm{d}F}{\mathrm{d}u} = 0, \quad \text{for} \quad u = u_m. \tag{2.6}$$

The displacement u_m corresponding to the maximum attainable force f_m is the physically meaningful solution of the equation

$$P(u_m) + u_m p(u_m) - 1 = 0. \tag{2.7}$$

The maximum force to which the system can be subjected is from (2.2) and (2.7)

$$F_m = Ku_m^2 p(u_m). \tag{2.8}$$

Once the maximum load (2.8) is reached in a load-controlled experiment the extant links will

rupture in a cascade mode unable to carry the force released by the link failing at $F = F_m$.

In unloading the force–displacement relation is simply

$$F = K(1 - D_u)u, \tag{2.9}$$

where D_u = constant is the damage level reached at the point at which the unloading commenced (at the highest recorded force F, Fig. 2). Consequently, the system unloads along the current (secant) stiffness $\bar{K} = K(1 - D_u)$, i.e., along a line connecting the point at which the unloading started and the origin of the F–u space. After the unloading is completed no residual strain is retained in the system.

Consider as an example the Weibull distribution of link rupture strengths

$$p(f_r) = \frac{1}{ku_m}\left(\frac{f_r}{ku_m}\right)^{\alpha-1} \exp\left[-\frac{1}{\alpha}\left(\frac{f_r}{ku_m}\right)^{\alpha}\right], \tag{2.10}$$

with the corresponding cumulative probability as the damage variable

$$D = \int_0^{ku} p(f_r)\, df_r = 1 - \exp\left[-\frac{1}{\alpha}\left(\frac{u}{u_m}\right)^{\alpha}\right], \tag{2.11}$$

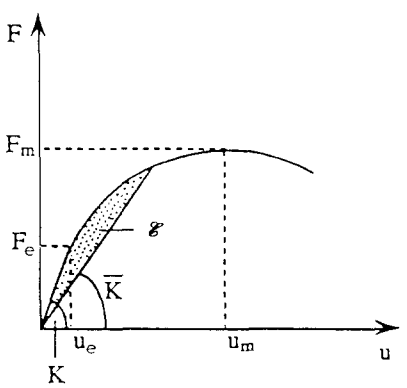

Fig. 2. The force–displacement relationship of the considered model. K is the initial elastic stiffness and $\bar{K} = K(1 - D)$ the current (damaged) elastic stiffness, (u_e, F_e) are the coordinates of the point at which damage commences, while (u_m, F_m) are the coordinates of the apex point separating the ascending and descending parts of the force–displacement curve. The dotted area represents the energy $\mathscr{E}$ used in the rupturing process.

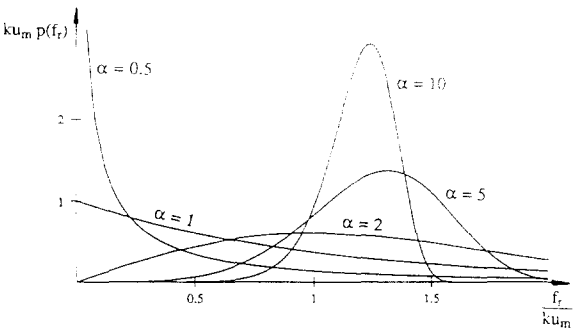

(a)

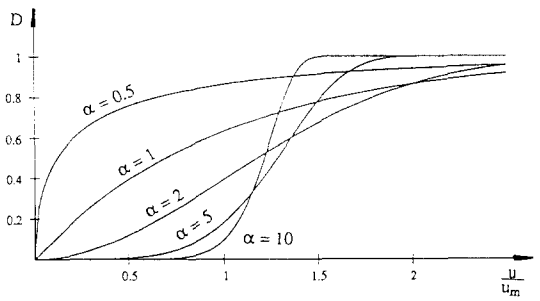

(b)

Fig. 3. (a) Weibull distribution of the link rupture strengths (Eq. (2.10)) plotted for five different values of the shape parameter α; (b) the corresponding cumulative probability, i.e., the damage parameter D (Eq. (2.11)), in function of displacement u.

where $\alpha > 0$ is the shape parameter. The plots of (2.10) and (2.11) for several values of α are shown in Fig. 3. The corresponding force–displacement relation is

$$F = Ku \exp\left[-\frac{1}{\alpha}\left(\frac{u}{u_m}\right)^{\alpha}\right]. \tag{2.12}$$

The maximum force is

$$F_m = F(u_m) = Ku_m \exp\left(-\frac{1}{\alpha}\right), \tag{2.13}$$

so that the shape parameter can be expressed in terms of macro parameters as $\alpha = \ln(Ku_m/$

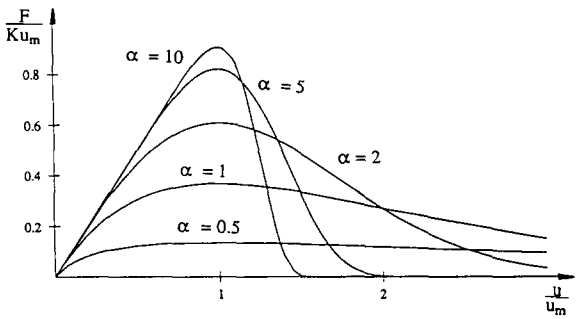

Fig. 4. The force–displacement curve corresponding to Weibull distribution, plotted for five different values of the shape parameter α. For large α, the behavior is of an elastic–perfectly brittle nature, while for smaller α behavior has a more "ductile" appearance.

$F_m)]^{-1}$. The damage corresponding to the maximum force is

$$D_m = 1 - \exp\left(-\frac{1}{\alpha}\right) = 1 - \frac{F_m}{Ku_m}. \tag{2.14}$$

The force–displacement curve, corresponding to (2.12), is depicted in Fig. 4 for five different values of the shape parameter. In function of the shape parameter α the force–displacement curve gives appearances of ductility or brittleness. For very high values of α the curvature of the force–displacement curve is very small and the failure occurs abruptly. In fact, for $\alpha \to \infty$, the Weibull distribution (2.10) becomes in the limit represented by a Dirac delta function

$$p(f_r) = \frac{1}{ku_m}\delta\left(\frac{f_r}{ku_m} - 1\right), \tag{2.15}$$

with the corresponding damage given by the unit step (Heaviside) function $D = H[(u/u_m) - 1]$. On the other hand, for example for $\alpha = 2$, the force–displacement curve has a shape characteristic of ductile deformation. In this case even the post-critical, or softening, segment of the curve is well developed predicting substantial displacements well beyond the displacement u_m corresponding to the apex of the force–displacement curve. As it is usually the case the actual nature of the response cannot be determined observing only the loading segment of the force–displacement curve. In each of the observed cases the unloading segment of the force–displacement curve always follows the straight line returning through the origin of the coordinate system.

In a certain number of cases the experimental results are fitted better with simpler functions. For example, micromechanical considerations indicate that the response of haversian (compact) bones are fitted better (Krajcinovic et al., 1987) by a single parameter distribution $p(f_r) = (f_{max})^{-1} = \text{constant}$, where f_{max} is the rupture strength of the strongest link. The parameter k/f_{max} can be readily written as a function of the macro variables. For example, in the present case $f_{max}/k = 2u_m$, where the index m denotes the value of the variable at the maximum force. Note also that the rupture strength of the link that ruptures at the maximum force $F = F_m$ is $f_r = f_{max}/2$. Therefore, all variables and parameters are in this case defined by a single, readily measured parameter u_m. In this case the ensuing force–displacement curve is a quadratic parabola

$$F = Ku\left(1 - \frac{ku}{f_{max}}\right) = Ku\left(1 - \frac{u}{2u_m}\right), \tag{2.16}$$

since the damage evolution law is from (2.4) and (2.5)

$$D = \frac{k}{f_{max}}u = \frac{u}{2u_m}, \qquad dD = \frac{k}{f_{max}}du = \frac{1}{2u_m}du. \tag{2.17}$$

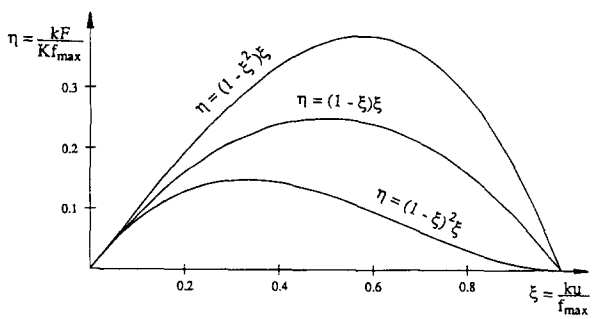

Fig. 5. The force–displacement curves corresponding to linearly ascending, constant and linearly descending rupture strength distributions.

Table 1
Maximum force, corresponding displacement and damage for linearly ascending, constant and linearly descending distributions of rupture strengths

Distribution	kF_m / Kf_{max}	ku_m / f_{max}	D_m
$p(f_r) = 2f_r / f_{max}^2$	$\frac{2}{3}\sqrt{3}$	$\frac{1}{3}\sqrt{3}$	$\frac{1}{3}$
$p(f_r) = 1/f_{max}$	$\frac{1}{4}$	$\frac{1}{2}$	$\frac{1}{2}$
$p(f_r) = 2(f_{max} - f_r)/f_{max}^2$	$\frac{4}{27}$	$\frac{1}{3}$	$\frac{5}{9}$

In this case, all system variables and parameters are defined by a single, readily measured parameter u_m. The linear damage evolution law (2.17) was suggested first in Janson and Hult (1977) and subsequently applied with a remarkable success for flexure of concrete beams (Krajcinovic, 1979) and long haversian bones (Krajcinovic et al., 1987). In the case of haversian bones the linear damage law was based on a convincing micromechanical argument.

Similar expressions can be readily derived for the case of a linearly ascending $p(f_r) = 2f_r/f_{max}^2$ and linearly descending $p(f_r) = 2(f_{max} - f_r)/f_{max}^2$ rupture strength distributions. The corresponding force–displacement curves are shown in Fig. 5. The maximum force F_m, corresponding displacement u_m and accumulated damage D_m are arranged in Table 1.

While the reason for this exercise will become apparent somewhat later in the text it suffices to indicate that none of the computed quantities is independent of the distribution of the link rupture strengths. In other words, the curvature of the force–displacement curve, existence of the post-critical (softening) region, accumulated damage and secant modulus corresponding to the apex of the force–displacement curve are strongly dependent on the microstructure. This is naturally to be expected.

3. Thermodynamic analysis

The energy $\mathscr{E}$ used on the rupture of links is equal to the difference between the mechanical work of the externally applied tensile force F and the energy of elastic deformation, that would be released in the course of subsequent unloading, i.e.,

$$\mathscr{E} = W - U = \int_0^u F \, du - \tfrac{1}{2} F u. \tag{3.1}$$

Geometrically, the energy $\mathscr{E}$ is equal to the area (dotted in Fig. 2) contained within the loading (ascending) and unloading (descending) segments of the force–displacement curve.

Consider the Helmholtz free energy of the entire system $\Phi = \Phi(u, D, T)$. Using the first law of thermodynamics and restricting considerations to isothermal processes (T = constant > 0), the rate of change of the free energy, during loading by monotonically increasing tensile force F, can be written in the usual form (Rice, 1978; Schapery, 1990)

$$\dot{\Phi} = F\dot{u} - T\Lambda, \tag{3.2}$$

where Λ is called the irreversible entropy production rate. The second law of thermodynamics requires that $\Lambda \geqslant 0$.

Let the free energy be equal to zero in the initial, unruptured and unloaded state ($D = 0$, $F = 0$). The free energy of a state defined by load $F > 0$ and damage $D > 0$ is then equal to the work done in transforming the body from its initial to current state along an imagined reversible and isothermal path. Following arguments analogous to those in Rice's (1978) related thermodynamic analysis of the quasi-static growth of Griffith cracks, a loaded state in which at least some of the links are ruptured ($D > 0$), can be created by an imagined sequence of two steps: first, $n = DN$ links are ruptured quasistatically pulling against the cohesive forces keeping together two adjacent layers of atoms, and second, stretching elastically the extant links until the requested state of deformation u is arrived at. The work associated with this sequence is

$$\Phi = E_\gamma + U, \tag{3.3}$$

where

$$E_\gamma = 2A \int_{\gamma_{min}}^{\gamma_r} \gamma_r p(\gamma_r) \, d\gamma_r, \tag{3.4}$$

is the energy of free surfaces created by rupturing n links, and γ_r is the link dependent specific surface energy. A denotes the initial unruptured cross-sectional area of the whole system. The linear elastic fracture mechanics suggests that the surface energy is a quadratic function of the force in the link at its rupture

$$\gamma_r = a f_r^2, \tag{3.5}$$

where a is a proportionality constant. Since $p(\gamma_r)\,\mathrm{d}\gamma_r = p(f_r)\,\mathrm{d}f_r$, (3.4) becomes

$$E_\gamma = 2aA\int_{f_{min}}^{f_r = ku} f_r^2 p(f_r)\,\mathrm{d}f_r. \tag{3.6}$$

The assumed quadratic relationship between γ_r and f_r, Eq. (3.5), is readily justified. Consider the deformation u at which a link, with the strength f_r, is at incipient rupture. The elastic energy of the link at incipient rupture is $\frac{1}{2}ku^2$. Assuming that, after rupture, λ part of this energy goes into the newly created surfaces,

$$\lambda \tfrac{1}{2} k u^2 = 2A_L \gamma_r, \tag{3.7}$$

where $2A_L$ is the ruptured surface area of the link. Since $ku = f_r$, from (3.7) it follows

$$\gamma_r = \frac{1}{4}\frac{\lambda}{kA_L} f_r^2, \tag{3.8}$$

from which the parameter a in (3.5) is $a = \lambda/4kA_L$.

Assuming the uniform distribution of link rupture strengths with finite band-width Δf

$$p(f_r) = \frac{1}{\Delta f}, \quad \Delta f = f_{max} - f_{min}, \tag{3.9}$$

from (2.4) the damage–displacement relationship is

$$D = \frac{ku - f_{min}}{\Delta f}. \tag{3.10}$$

Denoting by u_e the displacement at the beginning of damage accumulation, so that $f_{min} = ku_e$, (3.10) can be rewritten solely in terms of macroparameters as

$$D = \frac{u - u_e}{2u_m - u_e}. \tag{3.11}$$

The energy needed to form the free surfaces is derived substituting (3.9) into Eq. (3.6) and performing integration

$$E_\gamma = 2aA\left[f_{min}^2 D + f_{min}(\Delta f) D^2 + \tfrac{1}{3}(\Delta f)^2 D^3\right]. \tag{3.12}$$

Consequently, the Helmholtz free energy is obtained by substituting (3.12) into (3.3)

$$\Phi = \tfrac{1}{2}K(1-D)u^2 + 2aA\left[f_{min}^2 D + f_{min}(\Delta f) D^2 + \tfrac{1}{3}(\Delta f)^2 D^3\right]. \tag{3.13}$$

The rate of change of the free energy is therefore

$$\dot{\Phi} = \left[K(1-D)u\right]\dot{u} + \left\{-\tfrac{1}{2}Ku^2 + 2aA\left[f_{min} + (\Delta f) D\right]^2\right\}\dot{D}. \tag{3.14}$$

Comparing (3.14) and (3.2), it follows that $F = K(1-D)u$ and

$$TA = \left\{\tfrac{1}{2}Ku^2 - 2aA\left[f_{min} + (\Delta f) D\right]^2\right\}\dot{D}. \tag{3.15}$$

In view of (3.10) the above expression can be written as

$$TA = \left(\tfrac{1}{2}Ku^2 - 2aAk^2u^2\right)\dot{D}, \tag{3.16}$$

i.e., since $ku = f_r$ and $af_r^2 = \gamma_r$,

$$TA = \left(\tfrac{1}{2}Ku^2 - 2A\gamma_r\right)\dot{D}. \tag{3.17}$$

In (3.17) γ_r is the surface energy of the link rupturing at the displacement level u.

Introduce

$$\Gamma = -\frac{\partial U}{\partial D} = \tfrac{1}{2}Ku^2, \tag{3.18}$$

i.e., the energy release rate associated with the damage progression $\dot{D}$, as the driving force needed to rupture the links causing the damage, and

$$R = 2A\gamma_r, \tag{3.19}$$

as the current resistive force. Equation (3.17) and the requirement of a non-negative entropy production rate ($A \geqslant 0$) consequently give

$$(\Gamma - R)\dot{D} \geqslant 0. \tag{3.20}$$

Therefore, for continuing damage ($\dot{D} > 0$), it follows that $\Gamma - R \geqslant 0$, i.e., in order to continue damage, the damage driving force Γ must exceed the damage resistive force R. Expression (3.20) places a restriction on the constant λ, appearing in (3.8), requiring

$$\lambda \leqslant 1. \tag{3.21}$$

If the entire energy used in the rupturing process is transformed into the surface energy, $\lambda = 1$ and $\Gamma = R$.

4. Conjugate measures of damage and associated affinities

The rate of energy used in the rupturing process is from (3.1)

$$\dot{\mathscr{E}} = \dot{W} - \dot{U} = \left(F - \frac{\partial U}{\partial u} \right) \dot{u} - \frac{\partial U}{\partial D} \dot{D}. \tag{4.1}$$

Since $F = \partial U / \partial u$,

$$\dot{\mathscr{E}} = -\frac{\partial U}{\partial D} \dot{D} = \Gamma \dot{D}, \tag{4.2}$$

where Γ is the thermodynamic force or affinity conjugate to damage variable D. In view of

$$U = \tfrac{1}{2} F u = \tfrac{1}{2} K (1 - D) u^2, \tag{4.3}$$

it follows that

$$\Gamma = \tfrac{1}{2} K u^2, \tag{4.4}$$

as already established in (3.18). Geometrically, Γ is numerically equal to the area of the triangle doted in Fig. 6a. Physical interpretation of Γ becomes clear from the following argument. The quantity $\Gamma \, \mathrm{d}D$ is numerically equal to the dotted area of the small triangular strip shown in Fig. 6b, which is easily calculated to be

$$\Gamma \, \mathrm{d}D = \tfrac{1}{2} K u^2 \, \mathrm{d}D = \tfrac{1}{2} k u^2 \, \mathrm{d}n. \tag{4.5}$$

Hence, if $\mathrm{d}D$ corresponds to a single additional ruptured bar ($\mathrm{d}n = 1$), $\Gamma \, \mathrm{d}D$ is equal to the elastic energy of an individual link ($\frac{1}{2} k u^2$) released at the instant of its rupture.

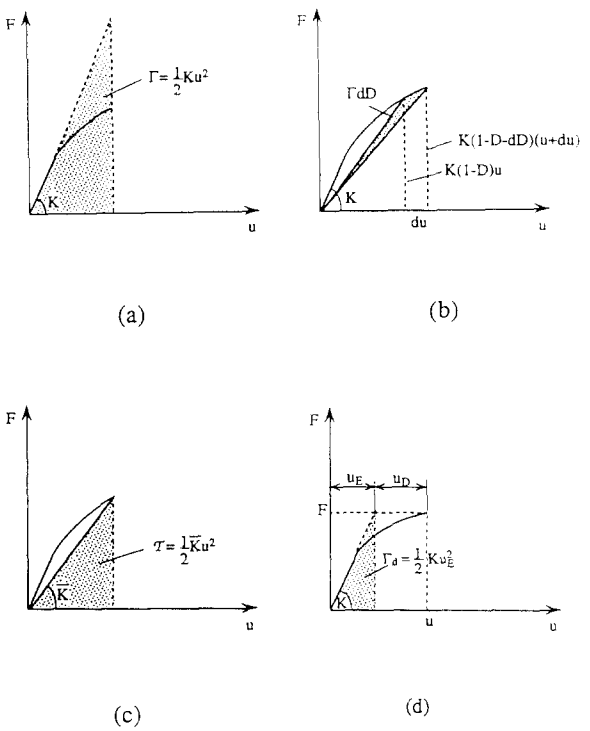

Fig. 6. (a) The thermodynamic force (affinity) Γ conjugate to damage variable D is represented by the area of the dotted triangle; (b) increment of the energy used in the rupturing process $\Gamma \, \mathrm{d}D$ is equal to the area of the dotted triangular strip; (c) the thermodynamic force (affinity) $\bar{\mathscr{F}}$ conjugate to logarithmic damage variable $\mathscr{D}$ is equal to currently available elastic energy equal to the area of the dotted triangle; (d) the thermodynamic force (affinity) Γ_d conjugate to damage variable d is equal to the strain energy associated with the elastic component of displacement u_E (area of the dotted triangle).

If the affinity Γ is expressed as a function of the damage variable $D = n/N$, given by (3.10), it follows

$$\Gamma(D) = 4 \frac{\Gamma_m}{f_{max}^2} \left[f_{min} + (\Delta f) D \right]^2. \tag{4.6}$$

The quantity

$$\Gamma_m = \tfrac{1}{2} K u_m^2 \tag{4.7}$$

denotes the value at the apex $u = u_m$, i.e., $\Gamma_m = \Gamma(D_m)$. In (4.7), $u_m = f_{max}/2k$ is the displacement corresponding to the maximum force, while $D_m = 0.5 \, (1 - f_{min}/\Delta f)$ is the associated damage. Note also that (4.6) can be expressed solely in

terms of macrovariables using $f_{\min}/f_{\max} = u_e/2u_m$, where u_e is the deformation at the onset of damage evolution.

The total energy used in the rupturing process from the initial state ($D = 0$) to the current state (with damage D) is

$$\mathscr{E} = \int_0^D \Gamma(D)\, \mathrm{d}D$$

$$= 4\frac{\Gamma_m}{f_{\max}^2}\left[f_{\min}^2 D + f_{\min}(\Delta f)D^2 + \tfrac{1}{3}(\Delta f)^2 D^3\right]. \tag{4.8}$$

In terms of macroparameters this can be rewritten as

$$\mathscr{E} = \Gamma_m\left[\left(\frac{u_e}{u_m}\right)^2 D + \frac{u_e}{u_m}\left(2 - \frac{u_e}{u_m}\right)D^2 + \frac{1}{3}\left(2 - \frac{u_e}{u_m}\right)^2 D^3\right]. \tag{4.9}$$

From (4.6)–(4.8), for $f_{\min} = 0$:

$$\Gamma = 4\Gamma_m D^2, \qquad \mathscr{E} = \tfrac{4}{3}\Gamma_m D^3. \tag{4.10}$$

Introduce now a new damage variable by defining its rate of change relative to the current number of the unruptured links $(N - n)$

$$\dot{\mathscr{D}} = \frac{\dot{n}}{N - n}. \tag{4.11}$$

Integrating (4.11) from the initial ($n = 0$) to the current state ($n > 0$), it follows that

$$\mathscr{D} = \ln\frac{N}{N - n}. \tag{4.12}$$

The logarithmic measure (4.12) was first used by Janson and Hult (1977). In analogy with the strain measure commonly used in the theory of plasticity, damage variable (4.12) can be referred to as a logarithmic damage. Since $0 \leqslant n \leqslant N$, it follows that $0 \leqslant \mathscr{D} \leqslant \infty$. Recall that the previous damage variable $D = n/N$ is defined in the interval $0 \leqslant D \leqslant 1$. The relations between the two measures of damage $\mathscr{D}$ and D are evident from

$$\mathscr{D} = -\ln(1 - D) = D + \tfrac{1}{2}D^2 + \tfrac{1}{3}D^3 + \cdots, \tag{4.13}$$

$$D = 1 - \exp(-\mathscr{D}) = \mathscr{D} - \tfrac{1}{2!}\mathscr{D}^2 + \tfrac{1}{3!}\mathscr{D}^3 - \cdots. \tag{4.14}$$

Their rates are related as:

$$\dot{\mathscr{D}} = \frac{1}{1 - D}\dot{D}, \qquad \dot{D} = \exp(-\mathscr{D})\dot{\mathscr{D}}. \tag{4.15}$$

Using the initial unruptured area A and current unruptured area $\bar{A} = (1 - D)A$, the introduced damage variables and their rates can be expressed as

$$D = \frac{A - \bar{A}}{A}, \quad \dot{D} = -\frac{\dot{\bar{A}}}{A}, \tag{4.16}$$

$$\mathscr{D} = \ln\frac{A}{\bar{A}}, \qquad \dot{\mathscr{D}} = -\frac{\dot{\bar{A}}}{\bar{A}}. \tag{4.17}$$

For infinitesimally small accumulated damages ($n \ll N$, $D \ll 1$), the distinction between two damage measures disappears, i.e., $\mathscr{D} \approx D$ and $\dot{\mathscr{D}} \approx \dot{D}$.

The thermodynamic force (affinity) $\mathscr{T}$ conjugate to damage variable (flux) $\mathscr{D}$ is obtained from

$$\dot{\mathscr{E}} = \Gamma\dot{D} = \mathscr{T}\dot{\mathscr{D}}, \tag{4.18}$$

such that

$$\mathscr{T} = \exp(-\mathscr{D})\Gamma = (1 - D)\Gamma = \tfrac{1}{2}\bar{K}u^2. \tag{4.19}$$

In (4.19)

$$\bar{K} = \exp(-\mathscr{D})K = (1 - D)K, \tag{4.20}$$

is the current elastic stiffness of the system, reflecting the already recorded damage. Geometrically $\mathscr{T}$ is the area of the dotted triangle shown in Fig. 6c. It is, in fact, identically equal to currently available elastic energy U, i.e., $\mathscr{T} = U$.

The entropy inequality (3.20) can now be expressed in terms of the damage variable $\mathscr{D}$ as

$$(\mathscr{T} - \mathscr{R})\dot{\mathscr{D}} = \left(\tfrac{1}{2}\bar{K}u^2 - 2\bar{A}\gamma_r\right)\dot{\mathscr{D}}, \tag{4.21}$$

where $\mathscr{R} = 2\bar{A}\gamma_r$ is the corresponding resistance force, while $\bar{A}$ is the cross-sectional area currently available to carry the external applied tensile force. For continuing damage ($\dot{\mathscr{D}} > 0$), (4.21) therefore requires $\mathscr{T} \geqslant \mathscr{R}$. If the entire energy used in the rupturing process is transformed into the free surfaces, $\mathscr{T} = \mathscr{R}$.

Other measures of (large) damage and conjugate affinities can be introduced, similarly as in large strain continuum mechanics (Hill, 1978). For example, the "Lagrangian type" damage can be defined by

$$D_L = \frac{A^2 - \bar{A}^2}{2A^2} = \frac{N^2 - (N-n)^2}{2N^2}$$
$$= \frac{n}{N} - \frac{1}{2}\left(\frac{n}{N}\right)^2 = D - \tfrac{1}{2}D^2. \tag{4.22}$$

Similarly, introduce a damage variable

$$d = \frac{A - \bar{A}}{\bar{A}} = \frac{n}{N-n}\left(= \frac{D}{1-D}\right), \tag{4.23}$$

as the number (n) of ruptured bars per current number of unruptured bars ($N-n$). The "Eulerian type" damage parameter can be then defined as

$$D_E = \frac{A^2 - \bar{A}^2}{2\bar{A}^2} = \frac{N^2 - (N-n)^2}{2(N-n)^2}$$
$$= \frac{n}{N-n} + \frac{1}{2}\left(\frac{n}{N-n}\right)^2 = d + \tfrac{1}{2}d^2. \tag{4.24}$$

The affinities conjugate to D_L and D_E follow from (4.18):

$$\Gamma_L = \frac{1}{1-D}\Gamma,$$
$$\Gamma_E = \frac{1}{1+d}\Gamma_d, \tag{4.25}$$

where $\Gamma_d = (1-D)^2\Gamma$ is the affinity conjugate to damage variable d. If the total displacement u is decomposed into its elastic and damage part by defining elastic component of displacement as displacement that would correspond to current force if no damage was produced ($u_E = F/K$, Fig 6d), then

$$u = u_E + u_D,$$
$$u_E = (1-D)u$$

and

$$u_D = Du. \tag{4.26}$$

The affinity Γ_d can then be expressed as

$$\Gamma_d = \tfrac{1}{2}Ku_E^2, \tag{4.27}$$

representing the accumulated strain energy associated with the elastic component of displacement u_E. Geometrically, Γ_d is equal to the dotted triangle shown in Fig. 6d.

5. Stability analysis of damage growth

It is of interest to examine the stability of the damage growth for displacement and force-controled tension tests. Assume, for simplicity, that energy used on the rupture process is transformed into the surface energy associated with newly formed surfaces, i.e., $\lambda = 1$ in (3.21). In this case the expression (3.12) for the entire surface energy acquires the following form

$$E_\gamma = \frac{K}{2k^2}\left[f_{\min}^2 D + f_{\min}(\Delta f)D^2 + \tfrac{1}{3}(\Delta f)^2 D^3\right]. \tag{5.1}$$

This expression is identical to (4.8) and can be rewritten solely in terms of macroparameters as in (4.9).

Consider first the displacement-controlled test. The potential energy of the system is then

$$\Pi_u(U, D) = U(u, D) + E_\gamma(D), \tag{5.2}$$

where

$$U(u, D) = \tfrac{1}{2}K(1-D)u^2 \tag{5.3}$$

is the macroscopically available elastic energy corresponding to state of deformation u and

damage D. The stationarity condition for the potential Π_u requires

$$\frac{\partial \Pi_u}{\partial D} = 0,$$

$$-\tfrac{1}{2}Ku^2 + \frac{K}{2k^2}\left[f_{\min}^2 + 2f_{\min}(\Delta f)D + (\Delta f)^2 D^2\right] = 0. \tag{5.4}$$

Equality (5.4) can be solved for D leading to the equilibrium condition

$$D = \frac{ku - f_{\min}}{\Delta f}. \tag{5.5}$$

Expression (5.5) is identical to the previously derived damage evolution law (3.10). To examine the stability nature of the equilibrium, it is necessary to derive the second derivative of the potential Π_u with respect to D

$$\frac{\partial^2 \Pi_u}{\partial D^2} = \frac{K}{k^2}(\Delta f)[f_{\min} + (\Delta f)D]. \tag{5.6}$$

Substitution of (5.5) into (5.6) leads to

$$\frac{\partial^2 \Pi_u}{\partial D^2} = \frac{K}{k}(\Delta f)u, \tag{5.7}$$

which is clearly positive for any positive value of the displacement u. Hence, in a displacement-controlled test the equilibrium damage growth is always stable. The plot of the potential energy Π_u (u, D) in function of the damage variable D, corresponding to several fixed values of displacement u, is shown in Fig. 7. For illustrative purposes it was assumed that $f_{\min} = 0$, allowing simpler representation

$$\Pi_u(u, D) = \tfrac{1}{2}Ku_m^2\left[(1-D)\left(\frac{u}{u_m}\right)^2 + \tfrac{4}{3}D^3\right]. \tag{5.8}$$

Consider next a force-controlled test. The potential energy in this case contains additionally the load potential term, i.e.,

$$\Pi_F = U(F, D) + E_\gamma(D) - Fu(F, D) = -\tfrac{1}{2}Fu(F, D) + E_\gamma(D). \tag{5.9}$$

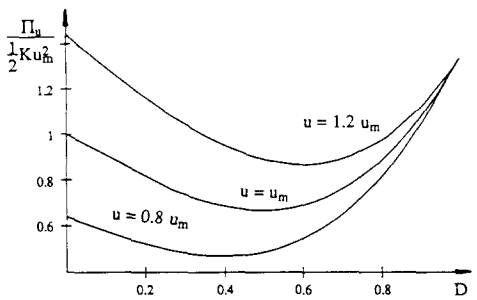

Fig. 7. Potential energy Π_u in a displacement-controlled test (Eq. (5.8)), plotted for three typical values of fixed displacement. The corresponding damage growth is always stable.

Substituting expression (5.1) for the surface energy and the relationship

$$u(F, D) = K^{-1}\frac{F}{1-D} \tag{5.10}$$

into (5.9) and performing requisite differentiation, the stationary condition requires

$$\frac{\partial \Pi_F}{\partial D} = 0,$$

$$-\tfrac{1}{2}K^{-1}\frac{F^2}{(1-D)^2} + \frac{K}{2k^2}\left[f_{\min}^2 + 2f_{\min}(\Delta f)D + (\Delta f)^2 D^2\right] = 0. \tag{5.11}$$

The equilibrium relationship between the force and corresponding damage is derived simplifying (5.11) to a form

$$F = \frac{K}{k}(1-D)[f_{\min} + (\Delta f)D]. \tag{5.12}$$

identical to the previously obtained expression (5.5). For given F, (5.12) is a quadratic equation for D. If

$$F < F_m = \frac{K}{k}\frac{f_{\max}^2}{4\,\Delta f} = K\frac{u_m^2}{2u_m - u_e}, \tag{5.13}$$

(5.12) has two real positive solutions, i.e, there are two equilibrium configurations. To examine the stability of two solutions, it is necessary to

evaluate the second derivative of the load potential with respect to the damage variable,

$$\frac{\partial^2 \Pi_F}{\partial D^2} = -K^{-1}\frac{F^2}{(1-D)^3} + \frac{K}{k^2}(\Delta f)[f_{\min} + (\Delta f)D]. \qquad (5.14)$$

using equilibrium condition (5.12), (5.14) can be conveniently written in the following form

$$\frac{\partial^2 \Pi_F}{\partial D^2} = -\frac{K}{k^2}(1-D)^{-1}[f_{\min} + (\Delta f)D] \times [f_{\min} + (\Delta f)(2D-1)]. \qquad (5.15)$$

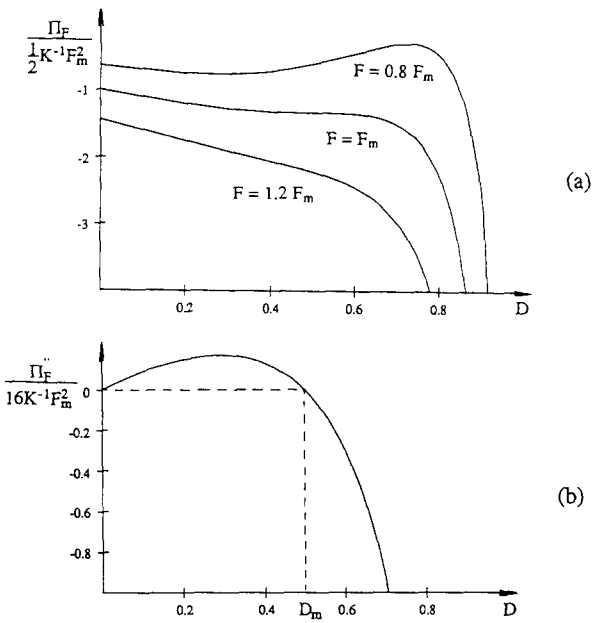

Fig. 8. (a) Potential energy Π_F in a force-controlled test (Eq. (5.17)), plotted for three typical values of the fixed force. For $F < F_m$, the potential energy has one minimum and one maximum, corresponding to the stable and unstable equilibrium configuration of the damaged state. For $F = F_m$ a single equilibrium state exists ($D = D_m = 0.5$) corresponding to the inflection point of the potential energy. For $F > F_m$, potential energy has no stationary value, since the force larger than F_m cannot be transmitted by the considered system. (b) The plot of the second derivative of the potential energy (Π_F'') in function of the the equilibrium values of damages variable D. For $D < D_m = 0.5$, $\Pi_F'' > 0$, indicating stable equilibrium configurations, while for $D > D_m = 0.5$, $\Pi_F'' < 0$, indicating unstable equilibrium configurations.

Consequently, equilibrium damage growth under the force-controlled test is stable as long as $f_{\min} + (\Delta f)(2D-1) < 0$, i.e., if

$$D < D_m,$$

$$D_m = \frac{1}{2}\left(1 - \frac{f_{\min}}{\Delta f}\right) = \frac{1}{2}\left(1 - \frac{u_e}{2u_m - u_e}\right). \qquad (5.16)$$

The other solution of (5.12) for which $D > D_m$, corresponds to unstable equilibrium, as the Hessian (5.15) becomes negative definite. This condition is satisfied along the descending (softening) part of the force–displacement curve. The plot of the potential energy $\Pi_F(F, D)$ as a function of the damage variable D, for several fixed values of the force F, is shown in Fig. 8a. Again, for illustrative purposes it is assumed that $f_{\min} = 0$, allowing the simple representation for Π_F

$$\Pi_F(F, D) = \frac{F_m^2}{2K}\left[-\left(\frac{F}{F_m}\right)^2 \frac{1}{1-D} + \frac{16}{3}D^3\right]. \qquad (5.17)$$

As seen in Fig. 8a, for $F < F_m$ the potential function Π_F has two stationary values. One is minimum and corresponds to stable configuration, while the other is maximum and corresponds to unstable configuration. For $F > F_m$ the potential energy Π_F has no stationary value, since forces larger than F_m cannot be transmitted by the considered system. The plot of the second derivative (5.15) versus equilibrium values of damage D is shown in Fig. 8b.

6. Damage resistance curve (*R*-curve)

An alternative way to examine and interpret the stability of damage growth is by introducing the notion of the damage resistance curve, analogous to the well-known resistance (R) curve of fracture mechanics (see, for example, Kanninen and Popelar (1985)). Consider the force-controlled test. Expression (5.17) can be rewritten as

$$\Pi_F(F, D) = \pi_F(F, D) + E_\gamma(D) = -\frac{F_m^2}{2K}\left(\frac{F}{F_m}\right)^2 \frac{1}{1-D} + \frac{F_m^2}{2K}\frac{16}{3}D^3, \qquad (6.1)$$

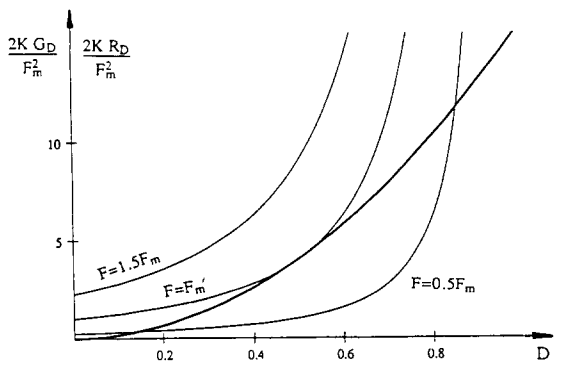

(a)

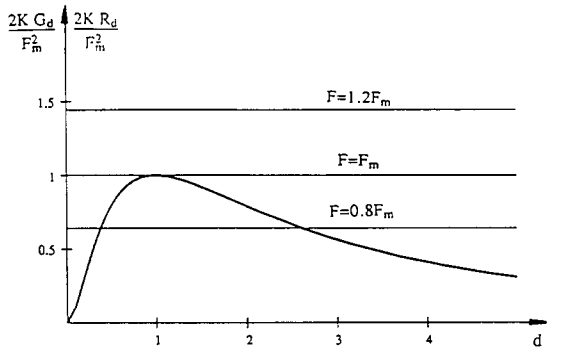

(b)

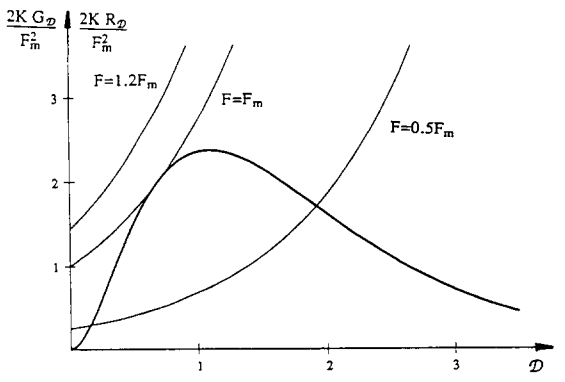

(c)

where $\pi_F(F, D)$ represents the sum of the elastic strain energy and load potential, while $E_\gamma(D)$ is the surface energy (5.9). The energy release rate due to the damage growth can be defined as

$$G(F, D) = -\frac{\partial \pi_F}{\partial D} = \frac{F_m^2}{2K}\left(\frac{F}{F_m}\right)^2 \frac{1}{(1-D)^2}, \tag{6.2}$$

while the damage resistance force is

$$R(D) = \frac{dE_\gamma}{dD} = \frac{F_m^2}{2K} 16D^2. \tag{6.3}$$

For a given force F, the accumulated damage is obtained from the equilibrium requirement

$$G(F, D) = R(D), \tag{6.4}$$

which leads to $F = 4F_m(1-D)D$, in agreement with (5.12), when $f_{min} = 0$. The corresponding state is the state of stable damage growth if, for a given force level, the rate of damage resistance force exceeds the rate of the energy release

$$\frac{\partial G}{\partial D} < \frac{dR}{dD}, \tag{6.5}$$

i.e., if the slope of the R-curve is greater than the slope of the G-curve at the point of their intersection. In the opposite case, damage growth is unstable. In analogy with the fracture mechanics, the R-curve can be referred to as the damage resistance curve. The R- and G-curves plotted for several values of applied force F are shown in Fig. 9a. As seen from this figure at the force value $F = F_m$ there is only a single equilibrium damage value $D = 0.5$. At this point the G- and

Fig. 9. (a) Energy release rate (G) versus damage resistance (R) curve, plotted by heavy solid line. For $F < F_m$, the curves intersect at two points, corresponding to the stable and the unstable equilibrium configuration, respectively. For $F = F_m$, the G-curve is tangent to the R-curve at the point of stability transition $D = D_m$. For $F > F_m$, the curves do not intersect, since there is no equilibrium damage state at that level of the applied force; (b) same as in (a), but with (G, R)-curves expressed relatively to damage variable d; (c) same as in (a), but with (G, R)-curves expressed relatively to damage variable $\mathscr{D}$.

R-curves touch each other, sharing the common tangent. For $F > F_m$, curves do not intersect, which means that there is no equilibrium damage growth for that level of force. For $F < F_m$, curves intersect at two points, one with damage $D < 0.5$, the other with damage $D > 0.5$. However, at the point $D < 0.5$, the slope of the R-curve is greater than the slope of the G-curve, hence condition (6.5) is fulfilled, and the damage growth is stable. For $D > 0.5$, the slope of the R-curve is smaller than that of the G-curve. The rate of resistance force cannot balance the rate of energy release rate, and the corresponding equilibrium state is characterized by unstable damage growth.

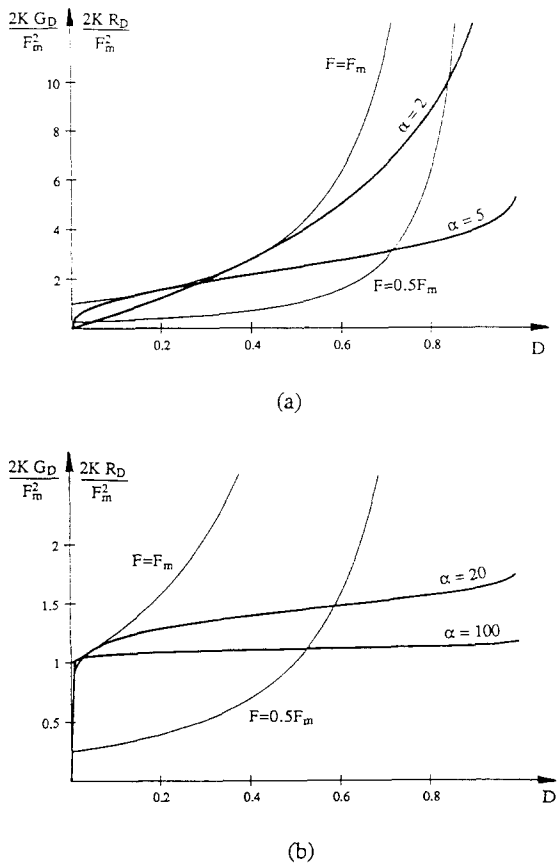

Fig. 10. (a) (G, R)-curves corresponding to Weibull distribution of rupture strengths. Two R-curves plotted correspond to two different values of the shape parameter α. (b) As $\alpha \to \infty$, the R-curve becomes nearly horizontal, as in the case of the well known Griffith criterion for homogeneous perfectly brittle solids.

It should be noted that in the considered model, the damage resistance curve is analytically determined because of known (assumed) rupture strength distribution, leading to corresponding expression for the surface energy of ruptured links (see (3.4) and (3.12)). Also, the shape of the R- and G-curves depends on the selected damage variable utilized in the analysis. For example, if the damage variable d was used instead of D, the (G, R)-curve is as shown in Fig. 9b. For a given force level, the energy release rate G_d turns out to be independent of d, so that G_d-curves become straight horizontal lines. Indeed:

$$G_d(F, d) = \frac{F_m^2}{2K}\left(\frac{F}{F_m}\right)^2,$$

$$R_d(d) = \frac{F_m^2}{2K} 16 \frac{d^2}{(1+d)^4}. \tag{6.6}$$

In this case the damage growth is stable below the damage value of $d = 1$, and is unstable above that value. Figure 9c shows (G, R)-curves expressed relative to the logarithmic damage variable $\mathscr{D}$.

If the Weibull distribution (2.10) was used instead of the constant rupture strength distribution, it readily follows that

$$\begin{aligned} \Pi_F(F, D) &= \pi_F(F, D) + E_\gamma(D) \\ &= -\frac{F_m^2}{2K}\left(\frac{F}{F_m}\right)^2 \frac{1}{1-D} \\ &\quad + \frac{F_m^2}{2K}(\mathrm{e}\,\alpha)^{2/\alpha} \\ &\quad \times \int_0^D (-\ln(1-D))^{2/\alpha}\,\mathrm{d}D, \end{aligned} \tag{6.7}$$

which replaces the previous expression (6.1). Since only the surface energy term E_γ is changed, the energy release rate is still given by (6.2), while the damage resistance force becomes

$$R(D) = \frac{\mathrm{d}E_\gamma}{\mathrm{d}D} = \frac{F_m^2}{2K}(\mathrm{e}\,\alpha)^{2/\alpha}\left(\ln\frac{1}{1-D}\right)^{2/\alpha}. \tag{6.8}$$

For example, for the shape parameters $\alpha = 2$ and $\alpha = 5$, corresponding R-curves are shown in Fig. 10a. Two typical G-curves (of course, both independent of α) are also shown. The damage value at which the damage growth ceases to be stable is $D = D_m$, given by (2.14). Clearly, as α becomes large, the Weibull distribution (i.e., in the limit, the Dirac delta function (2.15)) becomes more typical of the perfectly brittle behavior. The corresponding R-curve becomes similar to the Heaviside function (Fig. 10b), in agreement with the well-known Griffith criterion of the linear elastic fracture mechanics.

7. Tangent stiffness and system compliance

The work of the externally applied force done during the deformation process can be conveniently written as

$$W(u) = \int_0^u F(u)\,\mathrm{d}u = W_m - F_m u_m \left[\frac{2}{3} - \left(\frac{u}{u_m}\right)^2 + \frac{1}{3}\left(\frac{u}{u_m}\right)^3\right], \tag{7.1}$$

where

$$W_m = W(u_m) = F_m u_m \left[\frac{2}{3} - \frac{1}{6}\left(\frac{u_e}{u_m}\right)^3\right]. \tag{7.2}$$

Subscript m refers again to the point at which the force $F = F_m$ attains maximum, while index e refers to the point at which the force $F = F_e$ initiates the damage accumulation. In the case when all energy used in the rupturing process ($\mathscr{E}$) transforms into the surface energy (E_γ), the work W is exactly equal to corresponding free energy Φ, given by (3.3). The force–displacement relation is

$$F = \frac{\mathrm{d}W}{\mathrm{d}u} = F_m\left[2\frac{u}{u_m} - \left(\frac{u}{u_m}\right)^2\right], \quad u \geqslant u_e, \tag{7.3}$$

with the corresponding tangent stiffness

$$K_T = \frac{\mathrm{d}^2 W}{\mathrm{d}u^2} = \frac{2F_m}{u_m}\left(1 - \frac{u}{u_m}\right), \quad u \geqslant u_e. \tag{7.4}$$

At $u = u_e$ there is a discontinuity in the value of the tangent stiffness (modulus), from K during $u < u_e$, to $K - \Delta K_e$ immediately after $u = u_e$, where

$$\Delta K_e = K\frac{u_e}{2u_m - u_e}, \tag{7.6}$$

is the jump discontinuity due to initiation of the damage. Likewise, the jump discontinuity between the unloading (secant) modulus $\bar{K}$ and current tangent modulus K_T is $\Delta K = Ku/(2u_m - u_e)$. Note also that for $F = 0$, (7.3) gives the corresponding displacement $u = 2u_m$, i.e., $u = f_{max}/k$, as it should be, since the last link that ruptures has the strength f_{max}.

The complementary work of the externally applied force ($F < F_m$) is likewise

$$W^*(F) = \int_0^F u(F)\,\mathrm{d}F = W_m^* - F_m u_m\left[1 - \frac{F}{F_m} - \frac{2}{3}\left(1 - \frac{F}{F_m}\right)^{3/2}\right], \tag{7.7}$$

where $W_m^* = F_m u_m - W_m$ is the Legendre transform of W_m. The displacement–force relationship is

$$u = \frac{\mathrm{d}W^*}{\mathrm{d}F} = u_m\left[1 - \left(1 - \frac{F}{F_m}\right)^{1/2}\right], \quad F \geqslant F_e. \tag{7.8}$$

The system tangent compliance, being the second derivative of the complementary work

$$\frac{1}{K_T} = \frac{\mathrm{d}^2 W^*}{\mathrm{d}F^2} = \frac{u_m}{2F_m}\left(1 - \frac{F}{F_m}\right)^{-1/2}, \quad F \geqslant F_e, \tag{7.9}$$

becomes singular at the apex $F = F_m$ of the force–displacement curve, indicating zero tangent stiffness and infinite compliance there. The descending segment of the force–displacement curve, beyond $F = F_m$ corresponds to a distinctly different behavior on the microscale. The simple analysis, adequate to describe the ascending part of the force–displacement curve, cannot be successfully used for the descending part. The interaction of the microdefects during the descending (softening) part of the response significant rendering the assumption of the equal forces in all links unjustified. To account for the microdefect interaction it becomes necessary to introduce statistics of the spatial distribution of defects so that neither (7.3) nor (7.4) are likely to be appropriate.

In the case of the Weibull distribution of link rupture strengths (2.10), the force–displacement relation is given by (2.12). The corresponding stiffness is

$$K_T = \frac{F_m}{u_m}\left[1 - \left(\frac{u}{u_m}\right)^{\alpha}\right] \exp\left\{\frac{1}{\alpha}\left[1 - \left(\frac{u}{u_m}\right)^{\alpha}\right]\right\}. \tag{7.10}$$

Clearly, $K_T = 0$ at $u = u_m$. Also, for $u < u_m$, $K_T \to K = F_m/u_m$ when $\alpha \to \infty$, leading to elastic–perfectly brittle behavior with the linear force–displacement relation $F = Ku$.

8. Discussion and conclusions

The tenor of this study is derived from the major premise of micromechnical modeling. All micromechanical parameters must have a well-defined physical meaning. The macroparameters should be derived as volume averages of the corresponding microparameters. Transport parameters on the macroscale should reflect appropriately averaged kinetics of the irreversible changes in the microstructure. Complex mathematical structures needed to replicate inelastic behavior of solids can often obfuscate some of the essential features of the considered phenomena. While the simplicity is not a merit in itself, a carefully selected simplification is useful in gaining a valuable insight into the physics of the phenomenon. Despite, or perhaps because, of its deceptively simple mathematical structure, the parallel bar model provides a wealth of information revealing some of the fundamental aspects of the macro deformation of brittle solids reflecting the cooperative phenomena on the microscale. It is, therefore, interesting to summarize some of the results which might prove useful in transition to more sophisticated, and computationally more intensive, analytical models.

In this study damage growth on the microscale is understood as a continuous and gradual increase in the number n of ruptured links. Macroscopically the same process is observed as the decrease of the specimen stiffness, or as suggested, diminution of the secant modulus. At a certain density of the gradually evolving damage on the microscale, the macro compliance becomes singular, resulting in an abrupt and qualitative change of the specimen response (from hardening to softening).

The simple artifice considered in this study indicates that the damage evolution law is a direct reflection of the distribution of rupture strengths (or fracture energy γ) characterizing energy barriers which define the microcracking pattern on the microscale. The peril associated with judging the extent of the ductility of a specimen by the curvature of the loading segment of force–displacement curve is apparent. Varying the distribution of fracture strengths $p(f_r)$ it was possible to replicate an entire range of curves, some of which appear ductile.

It is true that the curvature of the force–displacement curve translates into energy dissipated on inelastic changes of the microstructure. However, the energies consumed in brittle (microcracking) and ductile (slip) phenomena have a different effect on the mechanical response and an even more disparate consequence on the mechanical failure. The ductile changes of the microstructure can be eliminated by cycling or annealing while the brittle damage is, in most cases, of a more permanent nature.

The present study suggests a plethora of damage parameters. Each of these in a physically

justifiable manner defines the state of damage on the macroscale. All of these damage parameters are averaged over the volume of the system and are, therefore, useful only within the self-consistent regime of the deformation process. In other words, the selection of the most suitable damage parameter cannot be made solely on the basis of the investigation of the effective continua (see, for example, Kunin (1983) and Nemat-Nasser and Hori (1990)).

A conjugate thermodynamic force is derived for each of the suggested damage parameters. Its magnitude was related to measurable macroparameters such as force and/or displacement. The stability criteria are derived in form of the Griffith's criterion with resisting force R computed from the distribution of microstructural toughnesses.

It is important to emphasize the limitations of the study. By assuming that each extant link carries equal force, the present self-consistent model neglects the influence of the stress concentrations on the evolution of damage. Consequently, the present model is adequate for homogeneous materials and low to moderate defect concentrations. The sequel to this study addresses the effect of the unequal distribution of forces to define the limits of applicability of the effective continua models.

Acknowledgement

The authors gratefully acknowledge the financial support rendered by the research grant from the US Department of Energy, Office of Basic Energy Research, Division of Engineering and Geosciences to the Arizona State University.

References

Daniels, H.E. (1945), The statistical theory of the strength of bundles of threads. I, *Proc. R. Soc. (London) A 183*, 405–435.

Hill, R. (1978), Aspects of invariance in solid mechanics, in: C.-S. Yih, ed., *Advances in Applied Mechanics*, Vol. 18, Academic Press, NY, pp. 1–75.

Hult, J., and L. Travnicek (1983), Carrying capacity of fibre bundles with varying strength and stiffness, *J. Mec. Theor. Appl. 2*, 643–657.

Iwan, W.D. (1967), On a class of models for the yielding behavior of continuous and composite systems, *J. Appl. Mech. 34*, 612–617.

Janson, J. and J. Hult (1977), Fracture mechanics and damage mechanics – A combined approach, *J. Mec. Appl. 1*, 69–84.

Kanninen, M.F. and C.H. Popelar (1985), *Advanced Fracture Mechanics*, Oxford University Press, Oxford.

Krajcinovic, D. (1979), Distributed damage theory of beams in pure bending, *J. Appl. Mech. 46*, 592–596.

Krajcinovic, D. (1984), Continuum damage mechanics, *Appl. Mech. Rev. 37*, 1–6.

Krajcinovic, D. (1989), Damage mechanics, *Mech. Mater. 8*, 117–197.

Krajcinovic, D., and M.A.G. Silva (1982), Statistical aspects of the continuous damage theory, *Int. J. Solids Struct. 18*, 551–562.

Krajcinovic, D., J. Trafimow and D. Sumarac (1987), Simple constitutive model for a cortical bone, *J. Biomech. 20*, 779–784.

Kunin, I.A. (1983), *Elastic Media with Microstructure II*, Springer, Berlin, Germany.

Lubarda, V.A., D. Sumarac and D. Krajcinovic (1992), Hysteretic behavior of ductile materials subjected to cycling loads, in: J.-W. Ju, ed., *Recent Advances in Damage Mechanics and Plasticity*, ASME Publication, AMD-Vol. 132, New York, NY, pp. 145–157.

Nemat-Nasser, S. and M. Hori (1990), Elastic solids with microdefects, in: G.J. Weng, M. Taya and H. Abe, eds, *Micromechanics and Inhomogeneity*, Springer, New York, pp. 297–320.

Rice, J. (1978), Thermodynamics of the quasi-static growth of Griffith cracks, *J. Mech. Phys. Solids 26*, 61–78.

Schapery, R.A. (1990), A theory of mechanical behavior of elastic media with growing damage and other changes in structure, *J. Mech. Phys. Solids 38*, 215–253.